



HAL
open science

Stable 500 kW average power of infrared light in a finesse 35 000 enhancement cavity

X.-Y Lu, R Chiche, K Dupraz, F Johora, A Martens, D Nutarelli, Y Peinaud,
V Soskov, A Stocchi, F Zomer, et al.

► **To cite this version:**

X.-Y Lu, R Chiche, K Dupraz, F Johora, A Martens, et al.. Stable 500 kW average power of infrared light in a finesse 35 000 enhancement cavity. *Applied Physics Letters*, 2024, 124 (25), pp.251105. 10.1063/5.0213842 . hal-04624376

HAL Id: hal-04624376

<https://hal.science/hal-04624376v1>

Submitted on 21 Nov 2024

HAL is a multi-disciplinary open access archive for the deposit and dissemination of scientific research documents, whether they are published or not. The documents may come from teaching and research institutions in France or abroad, or from public or private research centers.

L'archive ouverte pluridisciplinaire **HAL**, est destinée au dépôt et à la diffusion de documents scientifiques de niveau recherche, publiés ou non, émanant des établissements d'enseignement et de recherche français ou étrangers, des laboratoires publics ou privés.

Stable 500 kW average power of infrared light in a finesse 35,000 enhancement cavity

Stable 500 kW average power of infrared light in a finesse 35,000 enhancement cavity

X.-Y. Lu,^{1,a)} R. Chiche,¹ K. Dupraz,¹ F. Johora,¹ A. Martens,¹ D. Nutarelli,¹ Y. Peinaud,¹ V. Soskov,¹ A. Stocchi,¹ F. Zomer,¹ C. Michel,² L. Pinard,² E. Cormier,³ J. Lhermite,⁴ X. Liu,⁵ Q.-L. Tian,⁵ L.-X. Yan,⁵ W.-H. Huang,⁵ C.-X. Tang,⁵ V. Fedosseev,⁶ E. Granados,⁶ and B. Marsh⁶

¹⁾Université Paris-Saclay, CNRS/IN2P3, IJCLab, 91405 Orsay, France

²⁾Laboratoire des Matériaux Avancés - IP2I, CNRS, Université de Lyon, Université Claude Bernard Lyon 1, F-69622 Villeurbanne, France

³⁾Laboratoire Photonique Numérique et Nanosciences (LP2N), UMR 5298, CNRS-IOGS-Université Bordeaux, 33400 Talence, France

⁴⁾Université de Bordeaux- CNRS-CEA, Centre Lasers Intenses et Applications (CELIA), 351 cours de la Libération F- 33405 Talence, France

⁵⁾Department of Engineering Physics, Tsinghua University, Beijing 100084, China

⁶⁾CERN, CH-1211, Geneva, Switzerland

(*Electronic mail: aurelien.martens@ijclab.in2p3.fr.)

(Dated: 23 May 2024)

Advances in laser technology over the past 25 years have been impressive, in particular for the Ytterbium technology where nowadays kW-class laser systems are available. This technology also led to the possibility to provide hundreds of kilowatts of laser power by the use of enhancement cavities. We report here on the demonstration of a stable 500 kW average laser power in a high-finesse enhancement cavity. It paves the way towards systems providing laser power in excess of 1 MW and opens the door to a breakthrough in a variety of future applications.

Enhancement Fabry-Perot cavities (EC) with high average power, in the range of hundreds of kilowatts, are used or planned to be used for many applications. For instance, the Laser Interferometer Gravitational-Wave Observatory (LIGO) at Hanford was recently operated at 380 kW average power with continuous wave laser¹. Plans for operation at 800 kW have been made². Operation with pulsed laser was demonstrated up to 350 kW³. Beyond that, the demonstration of Steady-State Microbunching in electron accelerator would allow to produce high peak and high average power of EUV radiation provided that megawatt scale of laser power can be obtained in EC⁴⁻⁶. Such progress would also be of interest for photoneutralization of deuterium for fusion energy experiments^{7,8}. Production of intense quasi-monochromatic X- and γ -ray beams by means of inverse Compton scattering has been enabled by the advent of laser technology and still profiting from advances in the field⁹⁻¹⁴. Similar laser systems can be used in hadronic accelerators to interact with ultrarelativistic partially stripped ion beams instead which would open-up a broader range of applications^{15,16}. These accelerator-based applications involve the use of EC with pulsed lasers. In this regime, it has been shown that up to 670 kW can be reached with a cavity with Sapphire input mirror in picosecond regime¹⁷. However no study of long-term stability in the pulsed regime was published above 350 kW^{3,18}. With a fused-silica coupler up to 400 kW was obtained with 250 fs laser pulses with mode deformations induced by the presence of relatively low-order degenerate high-order modes. These results were obtained with a moderate effective enhancement factor, defined as the ratio of intracavity and input power, of

about 1,270 at such high average power. The input power was 315 W in these experiments. A drop of the effective enhancement factor with power was also observed in this work¹⁷. In the present letter, we report on progress beyond these results demonstrating in particular an effective enhancement factor increased by a factor of six at four times lower input power. We further demonstrate that stable power can be obtained at such high power in an EC. This is particularly advantageous for reducing the cost of these systems which is mainly driven by the amplifier cost. Moreover, it suggests that by employing a more powerful amplifier or further increasing the enhancement factor of the cavity, the average power could reach 1 MW and beyond.

The setup, shown in Fig. 1, comprises a Ytterbium-doped bulk passively mode-locked laser oscillator MENHIR-1030 from Menhir Photonics AG lightly instrumented by two piezoelectric transducers (PZTs) for repetition rate adjustment. The input of one of them is low-pass filtered with a few Hertz bandwidth and thus dubbed *slow* PZT in the following. Pump current can also be set with 1 mA precision by software setting to optimize the carrier-envelope offset frequency^{19,20}. The laser oscillator generates 200 fs pulses of Fourier-transform limited bandwidth at 1030 nm with a pulse repetition rate of 160 MHz and 150 mW average power. The power spectral density of phase noise was measured by optical beating with a reference continuous wave laser at 1030 nm. The residual RMS frequency jitter of a comb line of the pulsed laser is thus measured to be less than 1 kHz in the range [100 Hz, 1 MHz]^{16,21,22}. The laser pulses are then stretched by means of a Chirped Volume Bragg Grating (CVBG), transported and injected into a fibre. Before being injected into the amplifier, the laser beam goes through an acousto-optic modulator which is a part of the feedback loop, and also allows a coarse tuning of the carrier-envelope offset frequency. It is

^{a)}Also at Department of Engineering Physics, Tsinghua University, Beijing 100084, China.

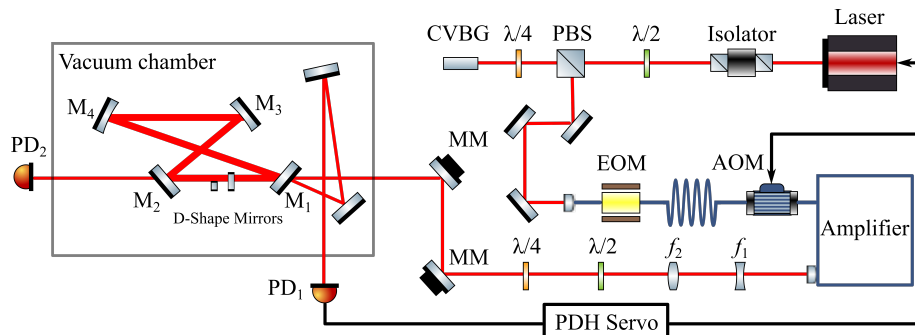


FIG. 1. Schematic of the experimental setup used during the experiments described in this letter. EOM stands for Electro-Optic modulator; AOM stands for Acousto-Optic modulator; PBS for polarizing beam splitter; CVBG for Chirped Volume Bragg Grating; PDH for Pound-Drever-Hall; PD for photodiode; MM for motorized mount.

followed by an electro-optic modulator that allows to produce an 8.3 MHz frequency modulation employed to lock the laser repetition rate and the free-spectral range (FSR) of the EC using the Pound-Drever-Hall technique²³. The laser light is then injected in a three-stage fibre power amplifier. It is operated in a saturated gain regime. Further details are documented elsewhere²². It delivers up to 75 Watts. The pulse duration is measured with a fast photodiode by carefully deconvoluting the response function of the photodiode measured directly with the sub-picosecond laser beam. It is estimated to be of approximately 160 ps FWHM. We decide not to compress the light pulses in order to avoid potential damage to the mirrors and study the influence of thermal effects. Pulse compression would involve a dedicated optimization of the cavity geometry to avoid working points close to the damage threshold of the mirrors²⁴. A telescope made of two fused-silica lenses mounted each on a manual translation and x-y adjusters is implemented to improve the mode matching to the EC. A pair of motorized mounts from Newport are used to align the laser beam to the EC. The EC is composed of four mirrors in a bow-tie configuration, typically tailored for Compton backscattering²⁵ and EUV applications²⁶. The FSR of the EC is set to 160 MHz. It is placed in a vacuum chamber pumped to about 10^{-2} mbar of residual pressure. It is composed of two planar mirrors, M_1 and M_2 , and two plano-concave mirrors, M_3 and M_4 , with radii of curvature of 500 mm. The beam radius at $1/e^2$ of intensity is measured to be about 1.0×1.2 mm behind M_2 , at a low average power, when the distance between the spherical mirrors is chosen to be about 505.0 mm. The distance in between the planar mirrors is set to 424.6 mm. Mirrors are mounted in thermal compensation mounts SU100TW-F2K from Newport. Two of them, M_1 and M_3 , are equipped with translation stages to tune the free spectral range of the cavity and the beam size on the mirrors.

In between the two planar mirrors (M_1 and M_2), D-shape mirrors are inserted to damp high-order modes that appear to be degenerate with the fundamental Gaussian mode at high

power¹⁸. The input coupling mirror M_1 is made of fused-silica and the design transmission in power of 115 parts per million (ppm). The coating of the three other mirrors, made of Ultra-low Expansion glass (ULE) substrate, is designed to maximize the reflectivity. One mirror from the same coating batch was measured to have a transmission of 1.75 ± 0.01 ppm. It has been measured by directing the output of the amplifier to the mirror and measuring the power in transmission carefully removing the contribution of diffracted light. To that end, the calibrated powermeter was placed at about a meter away from the mirror. As shown in Fig. 2, an excellent linearity of transmitted with respect to incident power is observed. This calibration procedure has also been employed for a mirror from the same batch of M_1 and the transmission measured to be of 113 ± 1 ppm, consistent with the design value. During experiments, the power has been measured in transmission of both M_2 and M_4 and found consistent within one percent. It provides both a sense of the accuracy with which the transmission power is measured and with which mirror transmission remains homogeneous over a given coating batch.

The intensity reflected by the EC was measured by the photodiode PD_1 and the signal is demodulated to provide an error signal using the Pound-Drever-Hall technique²³. It is then processed by a PID corrector to drive the *fast* PZT of the laser with a sensitivity of 4 Hz/V. The *slow* PZT voltage was adjusted manually in the range of 0-10 V though it could also be part of the feedback loop. This was not found necessary for the purpose of the demonstration reported in this letter. In order to avoid the *slow* PZT to get out of its driving range, we had to slowly and empirically adjust the linear translation of M_1 with a speed of 0.1 mm/s to preserve the locking for a long time. No loss of lock was observed while doing this. Again this operation was done manually without major difficulty and could be easily implemented in a software control to ensure an automatized procedure. In accelerator-based applications, this is of major importance since the FSR must be tuned to a harmonic of the revolution frequency of the particles in the accelerator²⁷. In practice, in such applications,

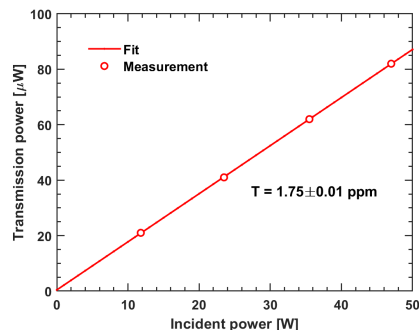


FIG. 2. Measured transmission versus incident power of a high reflectivity mirror taken from the same batch as $M_{2,3,4}$. The fitted transmission is found to be of 1.75 ± 0.01 ppm.

the cavity length is permanently tuned with a phase-locked loop by adjusting the voltage of a PZT implemented on M_2 of the optical cavity²⁷. Once the laser oscillator is locked onto the EC, its coupling must be optimized. This is made by improving the alignment, polarization, position of the lenses of the telescope (set on manual stages) and the pump current of the laser that allows to optimize the carrier-envelope offset frequency^{19,20}. Indeed it has been shown that if not optimized it induces an effective reduction of the effective enhancement factor²⁸. We have then operated the EC for a couple of weeks increasing gradually the amplifier power. The measurement of the power behind M_2 combined with the knowledge of the transmission of mirrors of this coating batch provides a measurement of the average power in the EC. The effective enhancement factor is thus measured to be 8,500. This quantity is the product of the coupling efficiency and the enhancement factor of the cavity determined by the losses in the optical cavity and the input mirror transmission. The direct measurement of the linewidth of the EC scanning the frequency of a sideband around 160 MHz of a continuous wave laser locked onto the EC provides a precise measurement of the finesse of 35300 ± 300 ²⁹. With the knowledge of the transmission of M_1 , it provides an estimation of the enhancement factor of 14,000.

We decided to make runs of ten minutes at several injection power P_i , see Fig. 3. It shows that we obtained more than 500 kW with excellent stability in the long term. This duration is only limited by our choice to stop the experiment not by any potential instability in the setup. Above 70 W of amplifier power, the operation limit of the amplifier is being reached, as seen by a significant rise of the pump diode temperatures. In order to preserve the hardware, we decided to reduce the run duration to five minutes. A very quick run at 75 W input power allowed us to measure 550 kW. Obtaining longer runs is only limited by the need to continue manually adjusting over the long term the cavity length. This presents no difficulty and is left for the next development stage towards automatization

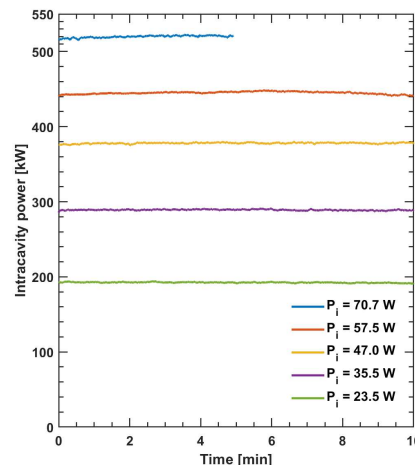


FIG. 3. Experimental measurements of intracavity power as a function of time for various values of injection power P_i .

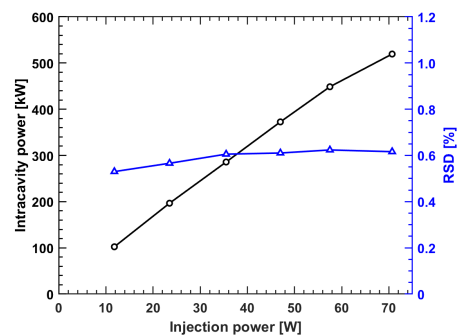


FIG. 4. Experimental measurements of the average intra-cavity power and its standard deviation relative to its average (RSD) as a function of injection power. Lines are drawn as a guide for the eye.

of the procedures. The measured power is shown in Fig. 4, where the standard deviation of the measured intensity relative to its average value (RSD) is shown. The fluctuations are found to be 0.6%.

We also measured the transverse mode of the EC by placing a beam profiler behind M_2 . The variation of the beam radius with intracavity power is demonstrated in Fig. 5. As expected, we observe an increase in the ellipticity with increasing power. In particular, the beam size is found to increase significantly in the sagittal plane and not in the tangential plane. When changing the distance between the spherical mirrors, the slope of the

This is the author's peer reviewed, accepted manuscript. However, the online version of record will be different from this version once it has been copyedited and typeset.

PLEASE CITE THIS ARTICLE AS DOI: 10.1063/5.0213842

Stable 500 kW average power of infrared light in a finesse 35,000 enhancement cavity

4

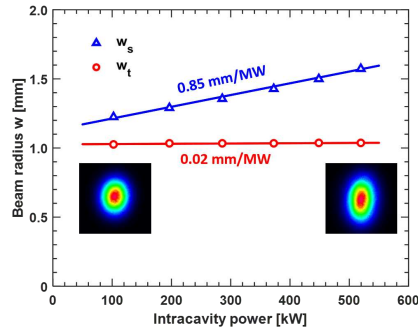


FIG. 5. Increase in the sagittal (w_s) and tangential (w_t) beam radius on cavity mode versus the intracavity power. The straight lines are linear fits. The beam profile snapshots taken at 102 kW and 520 kW are shown in the insets. From the simulation of the cavity, the estimated waist of the laser beam in between the spherical mirrors is $92 \times 71 \mu\text{m}$ at low power.

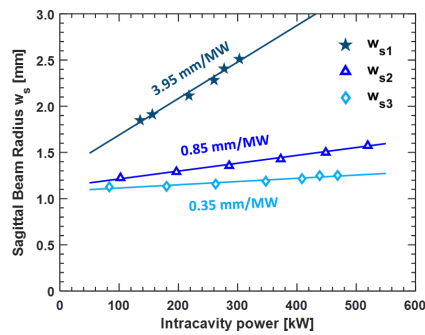


FIG. 6. Increase in the sagittal beam radius on cavity mode with respect to the intracavity power for three different cavity settings corresponding to a distance M_3M_4 of 503.3 mm (stars), 505.0 mm (triangles) and 506.1 mm (diamonds). The straight lines are linear fits. The estimated waists of the laser beam at low power in between the spherical mirrors are $74 \times 46 \mu\text{m}$, $92 \times 71 \mu\text{m}$ and $105 \times 80 \mu\text{m}$, respectively for the EC labelled 1, 2 and 3.

beam radius changes. This effect was already observed in the past and is related to the sensitivity of the mode size close to the instability region¹⁷. We do not intend to reproduce these results in detail, but we simply looked at this sensitivity for three different cavity settings, for which the distance between the spherical mirrors has been changed. The results are shown in Fig. 6. We also remark that the beam remains well modeled by the lowest order Gaussian intensity profile as suggested by the fit of the linecuts of the intensity profile at 102 kW and 520 kW, shown in Fig. 7.

Compared to the results at the state-of-the-art¹⁷, several

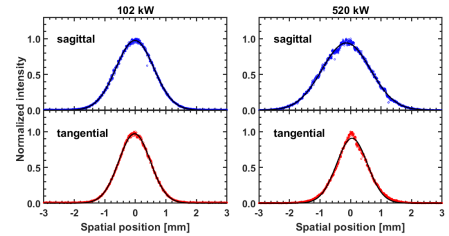


FIG. 7. Linecuts of the cavity mode at 102 kW (left panel) and at 520 kW (right panel) with corresponding Gaussian fits (solid lines) in the sagittal (top) and tangential (bottom) planes.

comments are in order. First of all, we provide a statement of the excellent stability of the laser power in the EC. We improve by a factor 2.5 our previous result of stable high average power in an EC¹⁸. Furthermore, we show in this letter that we extend the power enhancement beyond the 400 kW previously obtained with the similar setup of ULE mirrors with a fused-silica input coupler¹⁷. We also did not observe the detrimental effect of inclusions observed in previous coating series³⁰. We also did not observe a large effective enhancement factor degradation as found in Ref. 17. We attribute this to our ability to effectively damp higher-order modes¹⁸. In addition to the very high stability of the laser seeder, the good damping of high-order modes is also a reason for the excellent power stability observed. A slight degradation of the effective enhancement factor of 8,500 by approximately 10-15% comparing low and high average power is however experienced. This could be attributed to an inaccurate estimate of the coupling factor between low and high power or an actual increase of losses inside the EC related to the deformation of the optical surfaces due to thermal effects. Finite-element simulations coupled with a dedicated FFT code³¹ suggest that loss increase can be expected at a higher coating absorption level compared to that of the mirrors used for the experiments reported in this letter, estimated below 0.6 ppm^{32} . A quantitative and conclusive statement on this aspect is outside of the scope of this paper and kept for further studies.

The sensitivity of the beam profile due to a modification of topology of the cavity in the presence of residual thermal effects in the EC is unfortunately difficult to compare with those shown in Ref. 17. Indeed it is firstly sensitive to the cavity setting. We in particular show that the reported slopes of beam radius versus power obtained in this letter can be significantly smaller than that reported in the past, likely owing to a smaller absorption of the coatings. Compared to the results reported in the literature, the observed beam profile reported in this letter does not exhibit contributions from higher-order modes.

Last but not least, it must be noted that the results from

Ref. 17 are obtained with an EC with an effective enhancement factor of 2,000 (cold cavity, low power) and 1,270 (400 kW hot cavity), which is a factor four to six smaller than that reported in this letter. We observed that the performance of our setup is now restricted by the limited average power delivered by the amplifier that we are using. This limitation could be overcome by increasing the product of the cavity enhancement factor, the coupling efficiency and the input power. This could be done by (i) procuring a higher average-power amplifier, as nowadays available on the market; (ii) increasing the enhancement factor of the EC which would consist in finding a better optimum of the input mirror transmission and reducing overall losses of the EC. This could be possible owing to the very high stability of the laser seeder; (iii) further improving the mode matching to the EC. The first requires ensuring that amplification at higher power does not affect the phase noise properties of the laser significantly, which remains to be demonstrated. The second involves a reduction of overall losses in the EC, which likely implies further reducing the scattering losses of the mirror and thus improving the related surface quality. The last point might be slightly improved by a better optimization of the actual telescope, or by using for instance a more complicated telescope made of cylindrical lenses^{21,22}. It could also be better optimized by choosing a different working point where the beam spot size is less elliptical and less sensitive to the high average power. Overall the current results set a stage towards scalability towards 1 MW.

We have demonstrated that stable 500 kW power can be obtained in an enhancement Fabry-Perot cavity with a finesse of 35,000 and an effective enhancement factor of 8,500. We observed small but not limiting thermal effects at this level of power induced by the residual absorption in the coatings, at a level below one per million. The setup is mainly limited by (i) the enhancement factor that could be further increased (ii) the average power delivered by the amplifier. Commercially available industrial amplifier systems nowadays provide average power a factor of at least five larger than that used for this paper. It provides a clear path towards 1 MW and more average power in an enhancement cavity for applications as high-peak and high-average power sources of EUV radiation, X and γ rays. It also sets a stage for applications such as photoneutralization.

ACKNOWLEDGMENTS

The present work is partially financed by the French National Research Agency (ANR) under the Equipex program ANR-10-EQPX-0051. The authors also acknowledge the funding of CERN Physics Beyond Collider initiative. X.-Y. Lu stay at IJCLab was funded by National Key Research and Development Program of China (Grant No. 2022YFA1603403). The authors also acknowledge the support of the France-China Particle Physics Network which provided to the IJCLab and Tsinghua University teams a frame for fruitful exchanges over the past years.

DATA AVAILABILITY STATEMENT

The data that support the findings of this study are available from the corresponding author upon reasonable request.

- ¹D. Ganapathy, W. Jia, M. Nakano, *et al.* (LIGO O4 Detector Collaboration), "Broadband quantum enhancement of the ligo detectors with frequency-dependent squeezing," *Phys. Rev. X* **13**, 041021 (2023).
- ²J. Aasi, B. P. Abbott, R. Abbott, and others (The LIGO Scientific Collaboration), "Advanced ligo," *Classical and Quantum Gravity* **32**, 074001 (2015).
- ³B. S. Günther, *Storage Ring-Based Inverse Compton X-ray Sources: Cavity Design, Beamline Development and X-ray Applications* (Springer Nature, 2023).
- ⁴X. Lu, X. Liu, H. Wang, *et al.*, "High-power prototype optical enhancement cavity design for steady-state microbunching," in *Thirteenth International Conference on Information Optics and Photonics (CIOP 2022)*, Vol. 12478 (SPIE, 2022) pp. 9–16.
- ⁵Z. Li, X. Deng, Z. Pan, *et al.*, "Generalized longitudinal strong focusing in a steady-state microbunching storage ring," *Phys. Rev. Accel. Beams* **26**, 110701 (2023).
- ⁶X. Deng, A. Chao, J. Feikes, *et al.*, "Experimental demonstration of the mechanism of steady-state microbunching," *Nature* **590**, 576–579 (2021).
- ⁷A. Simonin, R. Agnello, S. Bechu, *et al.*, "Negative ion source development for a photoneutralization based neutral beam system for future fusion reactors," *New Journal of Physics* **18**, 125005 (2016).
- ⁸M. Tran, P. Agostinetti, G. Aiello, *et al.*, "Status and future development of heating and current drive for the eu demo," *Fusion Engineering and Design* **180**, 113159 (2022).
- ⁹O. Kulikov, Y. Telnov, E. Filippov, *et al.*, "Compton effect on moving electrons," *Physics Letters* **13**, 344–346 (1964).
- ¹⁰C. Bemporad, R. H. Milburn, N. Tanaka, *et al.*, "High-energy photons from Compton scattering of light on 6.0-gev electrons," *Phys. Rev.* **138**, B1546–B1549 (1965).
- ¹¹Z. Huang and R. D. Ruth, "Laser-electron storage ring," *Phys. Rev. Lett.* **80**, 976–979 (1998).
- ¹²I. Chaikovska, K. Cassou, R. Chiche, *et al.*, "High flux circularly polarized gamma beam factory: coupling a Fabry-Perot optical cavity with an electron storage ring," *Scientific Reports* **6**, 36569 (2016).
- ¹³B. Günther, R. Gradl, C. Jud, *et al.*, "The versatile X-ray beamline of the Munich Compact Light Source: design, instrumentation and applications," *Journal of Synchrotron Radiation* **27**, 1395–1414 (2020).
- ¹⁴K. Dupraz, M. Alkadi, M. Alves, *et al.*, "The thomx ics source," *Physics Open* **5**, 100051 (2020).
- ¹⁵M. W. Krasny, A. Abramov, S. E. Alden, *et al.* (GammaFactoryStudy-Group), "Gamma Factory Proof-of-Principle Experiment," Tech. Rep. (CERN, Geneva, 2019).
- ¹⁶A. Martens, K. Cassou, R. Chiche, *et al.*, "Design of the optical system for the gamma factory proof of principle experiment at the cern super proton synchrotron," *Phys. Rev. Accel. Beams* **25**, 101601 (2022).
- ¹⁷H. Carstens, N. Lilienfein, S. Holzberger, *et al.*, "Megawatt-scale average-power ultrashort pulses in an enhancement cavity," *Opt. Lett.* **39**, 2595–2598 (2014).
- ¹⁸L. Amoudry, H. Wang, K. Cassou, *et al.*, "Modal instability suppression in a high-average-power and high-finesse fabry-perot cavity," *Appl. Opt.* **59**, 116–121 (2020).
- ¹⁹A. Poppe, R. Holzwarth, A. Apolonski, *et al.*, "Few-cycle optical waveform synthesis," *Applied Physics B* **72**, 373–376 (2001).
- ²⁰S. A. Meyer, J. A. Squier, and S. A. Diddams, "Diode-pumped Yb:KYW femtosecond laser frequency comb with stabilized carrier-envelope offset frequency," *The European Physical Journal D* **48**, 19–26 (2008).
- ²¹P. Favier, *Etude et conception d'une cavité Fabry-Perot de haute finesse pour la source compacte de rayons X ThomX*, Theses, Université Paris-Saclay (2017).
- ²²L. Amoudry, *Etude de cavités Fabry-Perot de hautes finesse pour le stockage de fortes puissances moyennes. Application à la source compacte de rayons X ThomX*, Ph.D. thesis, Université Paris-Saclay (2021).
- ²³R. W. P. Drever, J. L. Hall, F. V. Kowalski, *et al.*, "Laser phase and frequency stabilization using an optical resonator," *Applied Physics B* **31**, 97–105 (1983).

This is the author's peer reviewed, accepted manuscript. However, the online version of record will be different from this version once it has been copyedited and typeset.

PLEASE CITE THIS ARTICLE AS DOI: 10.1063/1.50213842

- ²⁴H. Carstens, S. Holzberger, J. Kaster, *et al.*, "Large-mode enhancement cavities," *Opt. Express* **21**, 11606–11617 (2013).
- ²⁵F. Zomer, Y. Fedala, N. Pavloff, *et al.*, "Polarization induced instabilities in external four-mirror fabry-perot cavities," *Appl. Opt.* **48**, 6651–6661 (2009).
- ²⁶R. J. Jones and J. Ye, "Femtosecond pulse amplification by coherent addition in a passive optical cavity," *Opt. Lett.* **27**, 1848–1850 (2002).
- ²⁷J. Bonis, R. Chiche, R. Cizeron, *et al.*, "Non-planar four-mirror optical cavity for high intensity gamma ray flux production by pulsed laser beam Compton scattering off GeV-electrons," *Journal of Instrumentation* **7**, P01017 (2012).
- ²⁸A. Börzsönyi, R. Chiche, E. Cormier, *et al.*, "External cavity enhancement of picosecond pulses with 28,000 cavity finesse," *Appl. Opt.* **52**, 8376–8380 (2013).
- ²⁹C. R. Locke, D. Stuart, E. N. Ivanov, *et al.*, "A simple technique for accurate and complete characterisation of a Fabry-perot cavity," *Opt. Express* **17**, 21935–21943 (2009).
- ³⁰H. Wang, L. Amoudry, K. Cassou, *et al.*, "Prior-damage dynamics in a high-finesse optical enhancement cavity," *Appl. Opt.* **59**, 10995–11002 (2020).
- ³¹J. Degallaix, "Oscar a matlab based optical fit code," *Journal of Physics: Conference Series* **228**, 012021 (2010).
- ³²C. Comtet, D. Forest, P. Ganau, *et al.*, "Reduction of tantalum mechanical losses in Ta₂O₅/SiO₂ coatings for the next generation of VIRGO and LIGO interferometric gravitational waves detectors," in *42th Rencontres de Moriond - Gravitational Waves and Experimental Gravity* (La Thuile, Italy, 2007).